

## VIBRATION CONTROL OF AN OFFSHORE WIND TURBINE

Philip Alkhoury<sup>1</sup>, Mourad Aït-Ahmed<sup>1</sup>, Abdul-Hamid Soubra<sup>1</sup>, Valentine Rey<sup>1</sup>

<sup>1</sup>University of Nantes, France

Correspondence: Philip Alkhoury; Email: Philip.Alkhoury@etu.univ-nantes.fr

### ABSTRACT

*In order to reduce their cost, offshore wind turbines (OWTs) must have a powerful generator and a minimum overall weight. This has the consequence of making the OWT structure sensitive to dynamic excitations even at low frequencies. Indeed, modern multi-megawatt OWTs are composed of slender flexible and lightly damped components. The excessive vibrations of the OWT structure can impact the wind energy conversion to electricity, decrease the fatigue lifetime and even result in a total collapse of the structure when exposed to harsh environmental conditions. It is therefore important to reduce the unwanted vibrations of an OWT by implementing an appropriate control device that enhances its structural safety.*

*Motivated by the potential of the structural control methods in suppressing OWTs vibration, this paper proposes the design of a controlled active tuned mass damper (ATMD) system to reduce the nacelle/tower out-of-plane vibration of a monopile-supported 10 MW DTU OWT subjected to combined wave and wind loads. Compared to previous works, the main originality of this paper is the inclusion of a state estimator, Linear Quadratic (LQ) observer, within an optimal control schema. The state observer aims to drastically reduce the number of required system states. Indeed, as some measurements are practically impossible, all system states cannot be obtained. In this study, a fully coupled multi-degree of freedom (MDOF) analytical model of a monopile-supported OWT developed in [4] is used for this purpose. The optimal control schema makes use of the robust LQR feedback controller to establish the ATMD actuator control force. The developed active control schema proved to efficiently reduce the nacelle/tower vibration.*

Keywords: OWT, Structural control, vibration, ATMD, LQR, LQ observer

### 1. INTRODUCTION

Wind energy has received a vast global attention in recent years as being one of the most promising renewable energy resources. Considering the high and steady offshore wind speeds,

the onshore space limitations, and the less noise pollution in marine area, offshore wind turbines (OWTs) have gained more attraction than their onshore counterparts. However, compared to their onshore counterparts, OWTs experience excessive vibrations because of the simultaneous action of wind and wave loads, which significantly influence their design lifetime. Therefore, it is necessary to suppress the unwanted vibrations of the OWTs in order to ensure their safe operation.

Structural vibration control methods, which have been successfully employed in civil engineering structures, are a promising way to improve the dynamic response of OWTs. In recent years, the approach of applying vibration suppression devices to the OWT is an active area of research [1]. Three types based on the control strategy are usually considered: passive, semi-active, and active [1]. Passive control methods use constant parameters and do not require energy to function. A widely used representative example of the passive control system is a tuned mass damper (TMD) whose frequency is tuned to one of the target natural frequencies, primarily to the fundamental mode, to absorb vibrational energy. Recently, the passive TMD control approach has been implemented in wind turbine models for vibration reduction [2,3]. Compared to passive control systems, semi-active systems possess time-adjustable parameters tuned based on a feedback signal. Additional sensors, control algorithms and small amount of energy are required in this case [4, 5]. Finally, active control systems directly apply an active force to the passive vibration suppression device through a controlled actuator commanded by predefined algorithms. The control algorithm determines the active force from the structural displacements, accelerations, or other signals measured using sensors. A widely used example of an active control system is the active tuned mass damper (ATMD). Compared to the passive strategy, the active control approach can lead to a better mitigation of vibration although a certain amount of energy is required.

In spite of the fact that structural control strategies applied to OWTs are now gaining more attention in research, the application of ATMDs is still relatively new. In this scope [6, 7,

8, 9] proposed the use of an ATMD to study its potential in suppressing the out-of-plane (fore-aft) vibration of the OWT tower. The performance of the ATMD in vibration reduction is mainly governed by the choice of an appropriate control scheme. Different control algorithms have been proposed in literature such as  $H_\infty$  [10], static state feedback [8], linear quadratic LQ [6, 7, 9], etc. In the analysis by [10], the optimal control was derived by solving an  $H_\infty$  problem, which is conditionally stable and efficient when properly tuned. In the three studies by Fitzgerald et al. [6, 7, 9], effective vibration mitigation was derived on the basis of an optimal LQR control where all system states were measured to establish the actuator control force. In the scope of reducing the number of required measurements as not all system states are practically measurable, this study proposes the inclusion of a state estimator, Linear Quadratic (LQ) observer, within an optimal control schema, LQR controller.

In this paper, an ATMD control system is presented to suppress the nacelle/tower out-of-plane vibration of a monopile-supported 10 MW DTU OWT subjected to combined wave and wind loads. A fully coupled multi-degree of freedom (MDOF) analytical model of a monopile-supported OWT recently developed by Sun [4] was used for this purpose. The control force on the actuator was obtained using the robust LQR feedback controller combined with a Linear Quadratic observer. The MDOF as well as the control strategy were implemented in MATLAB/Simulink.

## 2. WIND TURBINE MODEL

In this study, the fully coupled MDOF analytical model of a monopile-supported OWT incorporating a TMD derived by Sun [4] is used. A brief description of this model is provided in the next section.

### 2.1 Description of the MDOF OWT analytical model

The equations of motion of the dynamic wind turbine model coupled with a TMD were established in [4] using the Euler-Lagrangian formulation expressed in Equation (1) below.

$$\frac{d}{dt} \frac{\partial T(t, q(t), \dot{q}(t))}{\partial \dot{q}_i(t)} - \frac{\partial T(t, q(t), \dot{q}(t))}{\partial q_i(t)} + \frac{\partial V(t, q(t))}{\partial q_i(t)} = Q_i(t) \quad (1)$$

Where  $T$  and  $V$  are the system kinetic and potential energy,  $q_i(t)$  is the displacement of the generalized degree of freedom (DOF)  $i$  and  $Q_i(t)$  is the generalized force corresponding to the  $i^{th}$  DOF. Sign  $(\dot{\phantom{x}})$  denotes the first derivative with respect to time.

Figure 1 illustrates the schematic model of the monopile-supported OWT with a TMD placed in the nacelle. The TMD is attached to the nacelle/tower to control the out-of-plane (fore-aft) nacelle vibration since the vibration in this direction is significantly larger than the side-to-side vibration. Figure 2 illustrates the coordinates of the blades (in-plane and out-of-plane), the nacelle and the TMD. The blades are modelled as continuous beams of variable mass and stiffness. In this simplified model, the soil effect is modeled by a translational spring with a constant stiffness coefficient  $k_x$  and a rotational spring with a constant stiffness coefficient  $k_\phi$  (Figure 3).

Similarly, soil damping is considered by two dashpots with constant damping coefficients  $c_x$  and  $c_\phi$  (Figure 3).

In total, the MDOF coupled analytical model contains 11 DOF, with  $q_1 - q_3$  representing the blade in-plane (edgewise) coordinates of the three blades,  $q_4 - q_6$  representing the out-of-plane (flapwise) coordinates,  $q_7 - q_8$  representing the nacelle fore-aft and side-side coordinates,  $q_9 - q_{10}$  representing the translational and rotational coordinates of the foundation and  $q_{11}$  denotes the relative coordinate of the TMD with respect to the nacelle. In the presented formulation, it has been assumed that the in-plane and out-of-plane displacements at any point  $r$  along the blade and at any point  $z$  along the tower are given in terms of the fundamental mode shapes ( $\phi_{1e}$ ,  $\phi_{1f}$  and  $\phi_{1t}$ ) and the generalized coordinates.

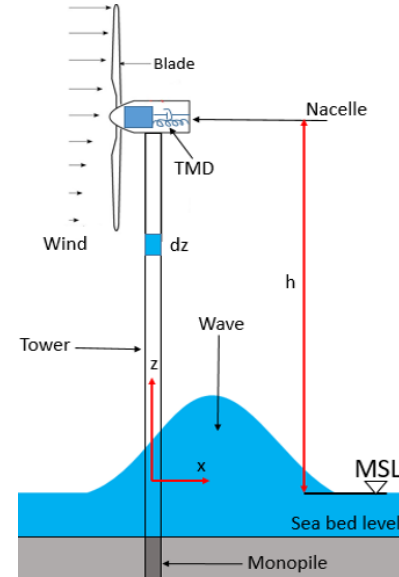


FIGURE 1: Monopile-supported OWT controlled by a TMD under wind and wave loadings (Modified based on Ref. [4]).

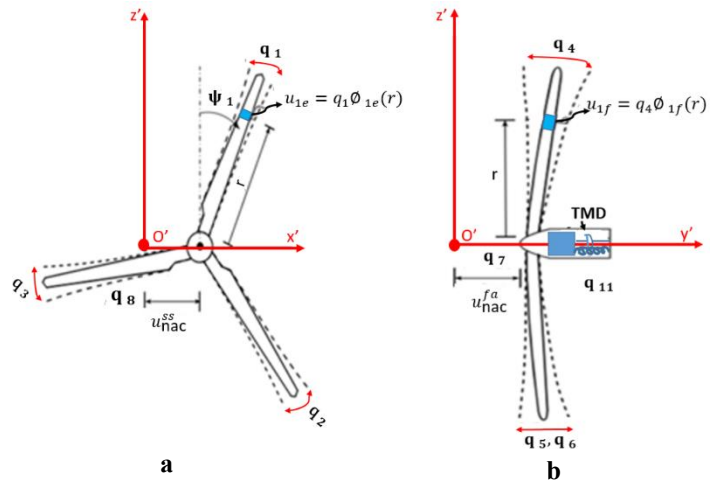
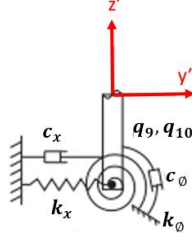


FIGURE 2: Displacements of the turbine blades, nacelle and TMD. (a) In-plane displacements; (b) Out-of-plane displacements (Modified based on Ref. [4]).



**FIGURE 3:** Simplified foundation model of the OWT (Modified based on Ref. [4]).

For consistency and due to space restrictions, only the motion of the nacelle (to which a TMD with a control scheme is applied) will be presented hereafter. The formulation of the blades motion and the tower velocity can be found in [4].

The absolute displacement of the nacelle (i) in the fore-aft direction  $u_{nac}^{fa}$  (Figure 2b) and (ii) in the side-side direction  $u_{nac}^{ss}$  (Figure 2a) are given as:

$$u_{nac}^{fa} = q_7 + q_9 + h \tan q_{10} \approx q_7 + q_9 + h q_{10} \quad (2)$$

$$u_{nac}^{ss} = q_8 \quad (3)$$

By deriving Equations (2) and (3), the absolute velocities in both directions can be found and the resultant velocity  $v_{nac}$  of the nacelle can be determined consequently as follows:

$$v_{nac}^{fa} = \dot{q}_7 + \dot{q}_9 + h \dot{q}_{10} \quad (4)$$

$$v_{nac}^{ss} = \dot{q}_8 \quad (5)$$

$$v_{nac} = \sqrt{(v_{nac}^{fa})^2 + (v_{nac}^{ss})^2} \quad (6)$$

The kinetic energy of the system with the TMD was found to be:

$$T = \frac{1}{2} \sum_{j=1}^3 \int_0^R \bar{m} v_{bj}(r, t)^2 dr + \frac{1}{2} M_{nac} v_{nac}^2 + \frac{1}{2} \int_0^h \bar{M} v_{tow}^2 dz + \frac{1}{2} M_f \dot{q}_9(t)^2 + \frac{1}{2} I_f \dot{q}_{10}(t)^2 + \frac{1}{2} m_{TMD} v_{TMD}(t)^2 \quad (7)$$

where  $M_{nac}$  is the mass of the hub/nacelle,  $M_f$  and  $I_f$  denotes the mass and moment of inertia of the foundation,  $\bar{m}$  and  $\bar{M}$  denote the mass density per unit length of the blade and the tower,  $m_{TMD}$  denotes the TMD mass,  $v_{bj}$ ,  $v_{tow}$  and  $v_{TMD}$  are the absolute velocities of the blade, the tower and the TMD respectively.

Similarly, the total potential energy  $V$  was given as:

$$V = V_b + \frac{1}{2} k_t^{fa} q_7^2 + \frac{1}{2} k_t^{ss} q_8^2 + \frac{1}{2} k_x q_9^2 + \frac{1}{2} k_\phi q_{10}^2 + \frac{1}{2} k_{TMD} q_{11}^2 \quad (8)$$

where  $V_b$  is the total potential energy of the blades,  $k_t^{fa}$  and  $k_t^{ss}$  denote the fore-aft and side-side stiffness of the tower,  $k_x$  and  $k_\phi$  denote the translational and rotational stiffness of the foundation and  $k_{TMD}$  denotes the stiffness of the TMD. Blades total potential energy  $V_b$  is found by considering the blades' strain energy due to bending, centrifugal stiffening effect and gravity [4, 6].

Substituting Equation (7) and Equation (8) back into Equation (1) gives the equation of motion for the simplified coupled OWT model with TMD and foundation. The equations of motion are of the form:

$$[M(t)]\{\ddot{q}\} + [C(t)]\{\dot{q}\} + [K(t)]\{q\} = \{Q\} + \{U_{atve}\} \quad (9)$$

$$\text{where } \{Q\} = \{Q_{wnd}\} + \{Q_{wve}\} \quad (10)$$

and  $[M(t)]$ ,  $[C(t)]$  and  $[K(t)]$  are the time-dependent system mass, damping and stiffness matrices respectively.  $\{Q_{wnd}\}$  and  $\{Q_{wve}\}$  are the generalized force vectors corresponding to wind and wave loadings.  $\{U_{atve}\}$  is the active control force vector which is defined later. The details of the system matrices are provided in [4] for reference.

Structural and aerodynamic damping of the blade (in the edgewise and flapwise directions) and of the nacelle/tower (in the fore-aft and side-side directions) were included in the equations of motion in the form of stiffness proportional damping [6].

### 3. ACTIVE CONTROL OF THE WIND TURBINE

In the present work, an ATMD is proposed to reduce the fore-aft tower vibrations. The tower top fore-aft velocity time history (Equation (4)) is chosen as the measurable input parameter for the control algorithm. The system matrices derived in Equation (9) are used for this purpose. Figure 4 shows a schematic of an ATMD system in the nacelle. The ATMD consists of a mass block, spring, damper and an actuator (hydraulic jack, worm drive, etc.).

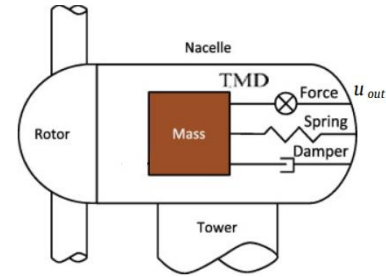


**FIGURE 4:** Schematic of an ATMD in the nacelle.

The generalized active control force vector  $\{U_{atve}\}$  (see Equation (9)), derived using the principle of virtual work, is expressed as:

$$\{U_{atve}\} = [\bar{B}]\{u_{out}\} \quad (11)$$

where  $\{u_{out}\}$  is the control force on the actuator connected to the TMD mass and  $[\bar{B}]$  is the control influence matrix given as:

$$[\bar{B}] = \begin{bmatrix} 0_{10 \times 1} \\ 1 \end{bmatrix} \quad (12)$$

The equations of motion are represented by a state-space model of order 22 as follows:

$$\begin{cases} \{\dot{\bar{q}}\} = [A]\{\bar{q}\} + [B]\{u_{out}\} + \{\overline{Q_{wnd}}\} + \{\overline{Q_{wve}}\} \\ \{y\} = [C]\{\bar{q}\} \end{cases} \quad (13)$$

$$\text{where } \{\bar{q}\} = \begin{Bmatrix} \{q\} \\ \{\dot{q}\} \end{Bmatrix}, [A] = \begin{bmatrix} 0_{11 \times 11} & I_{11 \times 11} \\ -M^{-1}K & -M^{-1}C \end{bmatrix},$$

$$[B] = \begin{Bmatrix} 0_{11 \times 1} \\ -M^{-1}[B] \end{Bmatrix}, \{\overline{Q}_{wnd}\} = \begin{Bmatrix} 0_{11 \times 1} \\ -M^{-1}Q_{wind} \end{Bmatrix}$$

$$\{\overline{Q}_{wav}\} = \begin{Bmatrix} 0_{11 \times 1} \\ -M^{-1}Q_{wave} \end{Bmatrix}, C = [0_{1 \times 17} \quad 1 \quad 0 \quad 1 \quad h \quad 0],$$

with  $0_{11 \times 11}$  and  $I_{11 \times 11}$  are the  $11 \times 11$  zero matrix and the  $11 \times 11$  identity matrix respectively,  $\{y\}$  being the output of the system to be controlled.

An appropriate control scheme is required to design the active vibration strategy. In this study, we propose an optimal control scheme to obtain the control force on the actuator  $\{u_{out}\}$ .

As stated above, in the previous studies by Fitzgerald [6, 7, 9], the control scheme makes use of the robust LQR feedback controller which is a very popular tool capable of operating a dynamic system at a minimum cost [11]. The same linear state LQR feedback is used in this study and it is given by:

$$\{u_{out}\} = [G_{LQR}]\{\bar{q}\} \quad (14)$$

where  $[G_{LQR}]$  is the LQR feedback gain and  $\{\bar{q}\}$  is the state vector. The optimal value for  $[G_{LQR}]$  is found by minimizing the tower displacement and control force using the cost function  $J_1$ :

$$J_1 = \min U_{atve} \left\{ \int_{t_0}^{t_f} [\{\bar{q}\}^T [Q] \{\bar{q}\} + \{U_{atve}\}^T [R] \{U_{atve}\}] dt \right\} \quad (15)$$

It should be noted that other cost functions with identical or even other control objectives (minimizing the variance of the tower deflection, minimizing the tower deflection velocity, etc.) can be used to find the optimal LQR feedback gain. Future work is planned to study the performance of different LQR controllers (different control objectives) in reducing the tower vibrations.

It should be mentioned that, the LQR design assumes that all the state variables  $\{\bar{q}\}$  are available for feedback (Equation (14)). However, in practice, not all state variables are measured. The reasons are that either this may not be physically feasible or that the sensors required are too expensive. In this paper, we propose an optimal control scheme which makes use of the robust LQR feedback controller combined with a Linear Quadratic (LQ) state observer (estimator). Figure 5 shows a block diagram of the controlled system with an LQR feedback controller only (Figure 5a) and with the combined LQR controller–observer (estimator) used in this work.

The LQ observer aims to reconstruct the complete state space information based on the measured output  $\{y\}$ , knowing the system description  $[A]$ ,  $[B]$  and  $[C]$ . The motivation behind the observer development is to provide the regulator with an estimation  $\{\hat{q}\}$  of the true state vector  $\{\bar{q}\}$  (Figure 5b). Consequently Equations (14) and (15) were modified by replacing  $\{\bar{q}\}$  by  $\{\hat{q}\}$ .

The state-space representation of the system with the observer is given as follows:

$$\begin{cases} \dot{\{\hat{q}\}} = [A]\{\hat{q}\} + [B]\{u_{out}\} + [L]\{y - \hat{y}\} \\ \{\hat{y}\} = [C]\{\hat{q}\} \end{cases} \quad (16)$$

where  $\{\hat{q}\}$  is the estimate of the actual state  $\{\bar{q}\}$ ,  $\hat{y}$  is the observer estimated output and  $[L]$  is the observer feedback gain.  $[L]$  is determined in such a way to minimize the observer estimation error  $\{\tilde{q}\} = \{\bar{q} - \hat{q}\}$ . The cost function to minimize for the optimal LQ observer is given as  $J_2$ :

$$J_2 = \min \left\{ \int_{t_0}^{t_f} [\{\tilde{q}\}^T [Q_e] \{\tilde{q}\} + \{\tilde{y}\}^T [R_e] \{\tilde{y}\}] dt \right\} \quad (17)$$

where  $\tilde{y} = \{y - \hat{y}\}$

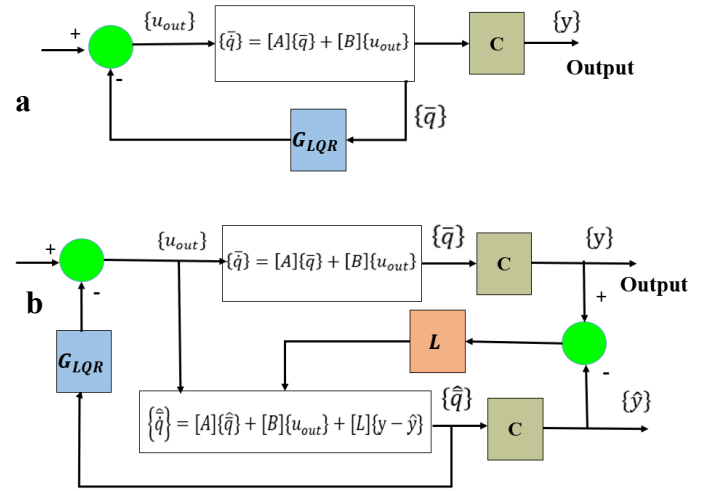


**FIGURE 5:** Block diagram of the controlled system (a) LQR feedback controller only, (b) combined LQR controller–observer (estimator) used in this work.

In Equations (15) and (17),  $[Q]$ ,  $[R]$ ,  $[Q_e]$  and  $[R_e]$  are weighting matrices used to put emphasize respectively on the states, control force, estimation error and the estimated output. Appropriate choice of the LQR weighting matrices ( $[Q]$ ,  $[R]$ ) is crucial in order to master the dynamics of the system states by using a minimum amount of energy. In this study, the weight  $[Q]$  has been set to the identity matrix, assigning, the same relative importance to the regulation of each state variable (i.e.  $[Q] = [I]_{22 \times 22}$ ). The weight on the control force  $[R]$  is assumed in the form  $[R] = \beta$  where  $\beta$  is a scalar. For the ATMD simulations, a sensitivity analysis was carried out and different controllers have been created by varying  $\beta$ . A value of  $\beta = 10^{-8}$  was found to ensure a good response reduction with acceptable control effort. Similarly, the observer weighting matrices,  $[Q_e] = [I]_{22 \times 22}$ ,  $[R_e] = 10^{-8}[I]_{1 \times 1}$  were found appropriate to ensure a minimum estimation error  $\{\bar{q}\} - \{\hat{q}\}$ .

#### 4. EXTERNAL LOADS

The external loads on the wind turbine model were determined using the NREL aero-servo elastic simulator FAST [12]. The aerodynamic loads were determined using the AeroDyn subroutine, which is based on the blade element

momentum theory. It considers the effects of axial and tangential induction and the tip and hub losses calculated using the Prandtl model. Moreover, the HydroDyn subroutine was applied to calculate the hydrodynamic loads acting on the supporting monopile.

## 5. NUMERICAL SIMUMATIONS

The effectiveness of the ATMD and the proposed control algorithm were evaluated in this section. The monopile-supported reference DTU 10 MW three-bladed OWT was used [13]. In this paper, the total length of the monopile was chosen as 80 m, in which 25 and 45 m are in the water and seabed, respectively, and another 10 m was added above the mean sea level corresponding to the transition piece. It should be noted herein that the soil-monopile system (monopile in soil of 45 m length) was replaced in the MDOF model by a translational and rotational spring at mudline. The fundamental mode shape (edgewise and flapwise) of the blade and the tower were computed using BModes [14] and are given in Equation (17) and Figure 6.

$$\begin{aligned} \phi_{1e}(\bar{r}) &= 0.06974 \bar{r}^6 - 0.7149 \bar{r}^5 + 0.4562 \bar{r}^4 + 0.828 \bar{r}^3 \\ &\quad + 0.362 \bar{r}^2 \\ \phi_{1f}(\bar{r}) &= -0.6245 \bar{r}^6 - 0.08439 \bar{r}^5 + 1.261 \bar{r}^4 + 0.1443 \bar{r}^3 \\ &\quad + 0.1351 \bar{r}^2 \\ \phi_t(\bar{z}) &= 0.1095 \bar{z}^6 - 0.3118 \bar{z}^5 - 0.4788 \bar{z}^4 + 1.6023 \bar{z}^3 \\ &\quad + 0.0785 \bar{z}^2 \end{aligned} \quad (17)$$

where  $\bar{r} = r/86.366$  and  $\bar{z} = z/150.63$  denote the normalized blade radius and tower height respectively.

The stiffness of the soil springs (Figure 3), were taken from [15] and those of the damping from [4]. Notice that in [15], the parameters of the simplified foundation model (a translational and a rotational spring) used in this study were derived from force-displacement curves obtained from three-dimensional finite element simulations. With reference to [15] and [4] values of  $k_x$ ,  $k_\phi$  and  $c_x (= c_\phi)$  were obtained as  $k_x = 2.48 \times 10^9$  N/m,  $k_\phi = 4.12 \times 10^{11}$  N.m/rad and  $c_x = c_\phi = 9.34 \times 10^8$  N.m.s/rad.

Table 1 below lists the modal frequencies for each DOF as obtained from an eigenanalysis performed on MATLAB based on the MDOF model of the DTU 10 MW. A comparison was made between the predicted modal frequencies from the MDOF model and those of the 3D FE model recently developed by the authors in [15]. By examining Table 1, we see that the results agree well which validates the use of the MDOF model for ATMD design.

In this study, the total mass of the out-of-plane TMD was assumed to be 2% of the total wind turbine mass and it is 40,263 kg based on the information provided in [13,15]. Note that the proposed TMD mass is around 6% of the total RNA mass. Further, the TMD was tuned to the tower's fundamental fore-aft frequency of 0.198 Hz (see Table 1) and an optimum tuning ratio  $\nu = 0.98$  was defined based on the expression given by [16]. A

damping ratio of  $\zeta = 7.2\%$  was used for the TMD. It was derived based on [17]. As a result, the TMD stiffness and damping coefficients adopted in this study were respectively 59,848 N/m and 7,069 N.s/m

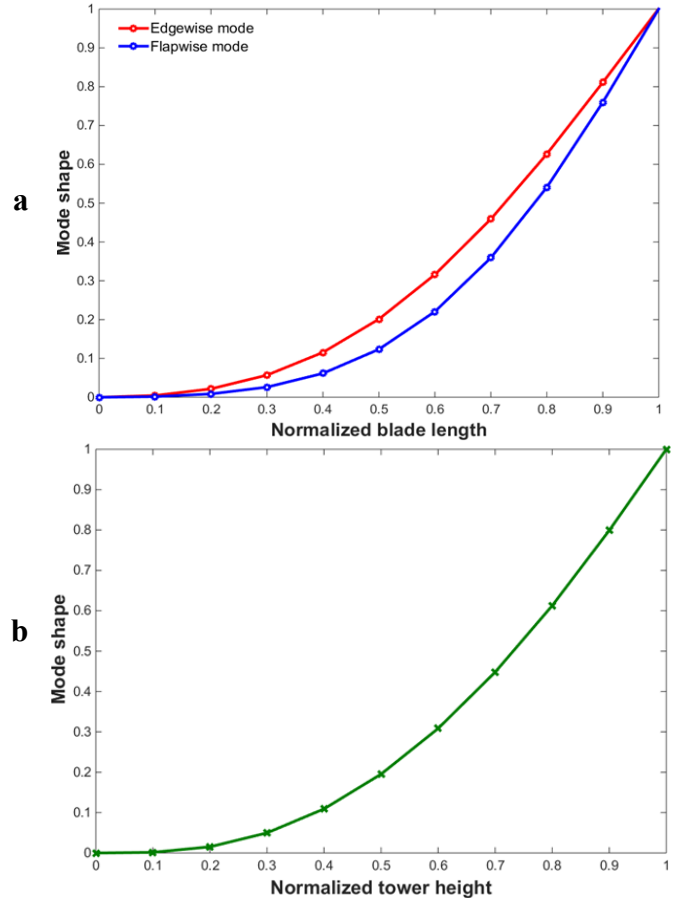


**FIGURE 6:** Fundamental mode shapes of the (a) blade and (b) tower.

Model	Blade in-plane (Hz)	Blade out-of-plane (Hz)	Tower side-to-side (Hz)	Tower Fore-aft (Hz)
[15]	0.932	0.544	0.201	0.202
MDOF	0.941	0.538	0.196	0.198

**TABLE 1:** Natural frequencies of the monopile-supported 10 MW DTU OWT as computed by the MDOF and the 3D FE model [15].

In order to get a realistic presentation of a typical offshore wind site, the wind and wave conditions from the reference Project UpWind [18] were used in this paper. This is an offshore wind site located in the Dutch North Sea, which is a typical site suitable for monopile foundations in shallow water depths. Load cases (LC) 4, 6 and 14 (with different wind speeds and operating conditions) were used in the present analyses and are shown in Table 2 below.

Load Cases	$U$ , (m/s)	$TI$ , (%)	$H_s$ , (m)	$T_p$ , (s)	$f$ , (%)
4	8	16	1.31	5.67	13.923
6	12	14.6	1.7	5.88	14.272
14	28	11.9	4.17	8.49	0.202

**TABLE 2:** Load cases considered in the analysis [18].

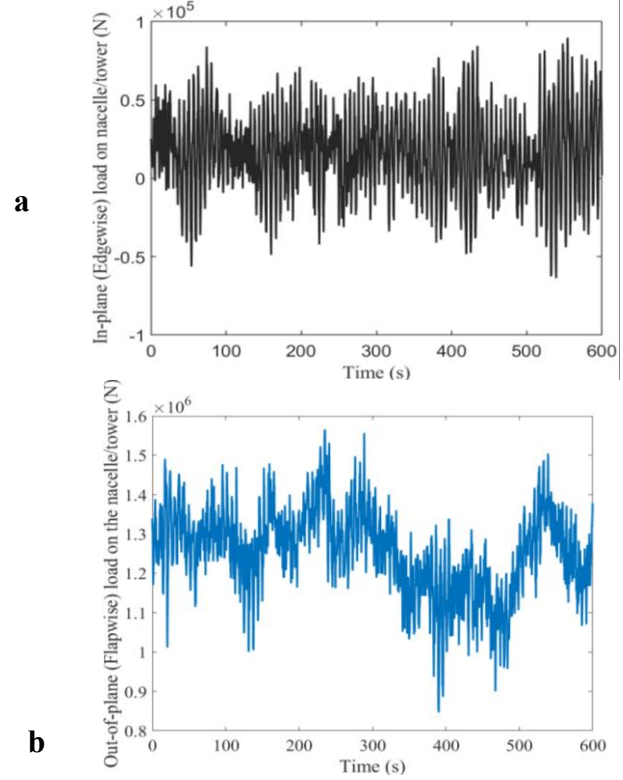
In Table 2,  $U$  is the mean wind speed at hub height,  $TI$  is the turbulence intensity,  $H_s$  is the significant wave height,  $T_p$  is the peak spectral period and  $f$ (%) is the frequency of occurrence of the load case. LC4 and LC6 from Table 2, where the mean wind is between cut-in (4 m/s) and cut-out (25 m/s) speed, represents DLC 1.2 Power production from IEC 61400-3, while LC14, with wind above cut-out speed applies to DLC 6.4 Parked (standing still or idling).

Figure 7a and 7b shows the generalized loads (wind and wave loads) for the generalized degree of freedom ( $q_7$  and  $q_8$ ) corresponding respectively to the in-plane and out-of-plane vibration of the nacelle/tower for LC6. Also, Figure 8a and 8b gives respectively the generalized aerodynamic loads for each generalized degree of freedom ( $q_1$ - $q_6$ ) corresponding to the edgewise and flapwise vibration of the blades for LC6. The generalized loads for other LCs were not presented herein due to space limitations.

The active control scheme is now tested to see if it can reduce the nacelle/tower vibration for the three LCs considered in this study. Figures 9, 10 and 11 illustrate the effect of the combined LQR controller-observer ATMD on the fore-aft tower top displacement for LC4, LC6 and LC14 respectively. From Figures 8, 9 and 10, it is clear that the developed control scheme applied to the ATMD shows excellent performance for different wind speeds and operating conditions. Tower top vibrations were greatly reduced, where peak-to-peak and root mean square (RMS) displacement reduction up to 21% and 30% were respectively achieved for LC4. The vibration reduction being much higher for LC6 (40% peak-to-peak and 67% RMS reduction) and LC14 (30% peak-to-peak and 44.5% RMS).

It should be noted that these impressive reductions of the OWT tower top response come at the expense of a very slight increase of the mass at the top of the tower. On one hand, this itself may sometimes results in a thicker tower, as tower thickness is governed by ultimate load calculation (ULS). On the other hand, the ATMD which proved its effectiveness in vibration reduction can help in mitigating the fatigue loads and thus resulting in the prolongation of the service lifetime of the OWT and in reducing the potential maintenance cost. This is a trade-off that must be considered during the design of a wind turbine.

Finally, future work is planned to investigate the mechanical (and power) requirements of the active system and feasible design options by considering realistic devices, actuators and control-structure interaction.



**FIGURE 7:** Generalized loads for the generalized degree of freedom ( $q_7$  and  $q_8$ ) corresponding to the (a) in-plane and (b) out-of-plane vibration of the nacelle/tower for LC6.

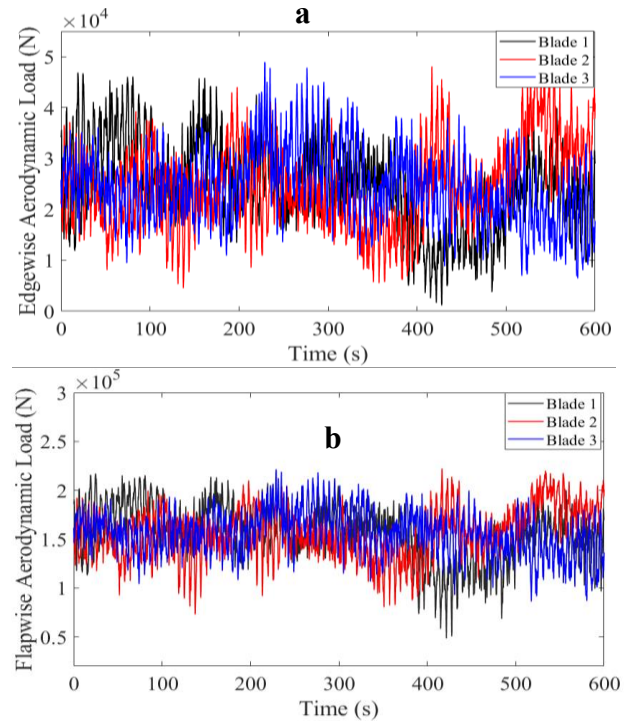


**FIGURE 8:** Generalized aerodynamic loads for each generalized degree of freedom ( $q_1$ - $q_6$ ) corresponding to the (a) edgewise and (b) flapwise vibration of the blades for LC6.

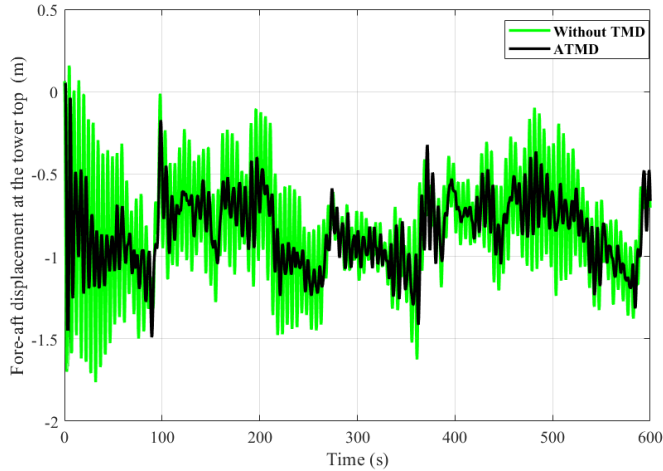


**FIGURE 9:** Fore-aft displacement of the tower in the presence of the proposed ATMD for LC4.

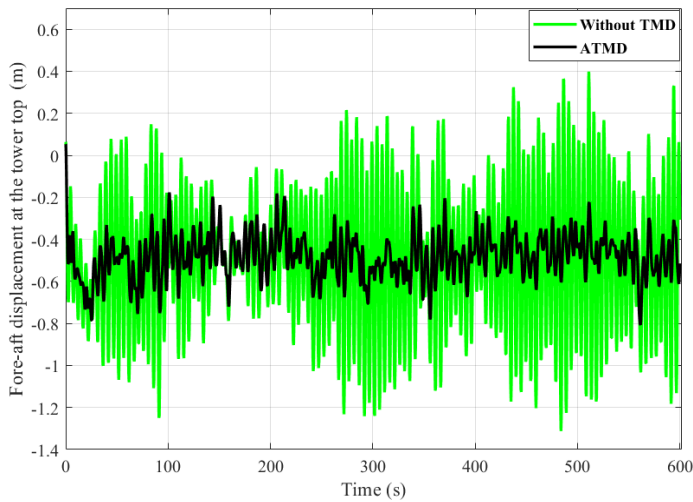


**FIGURE 10:** Fore-aft displacement of the tower in the presence of the proposed ATMD for LC6.

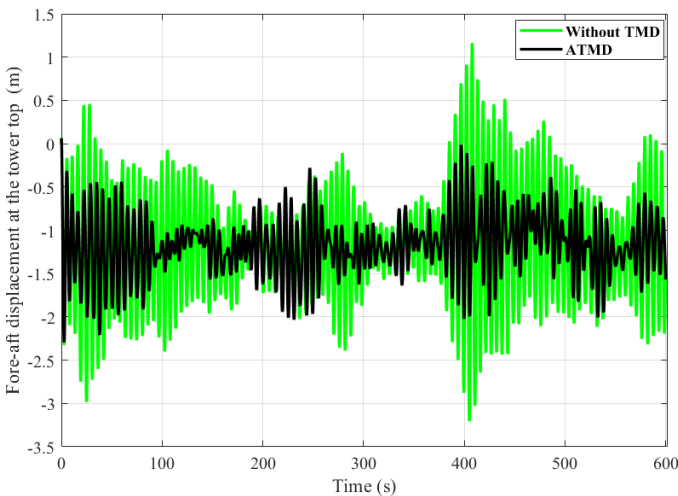


**FIGURE 11:** Fore-aft displacement of the tower in the presence of the proposed ATMD for LC14.

## CONCLUSION

In this paper, an 11 DOF analytical model for a monopile-supported offshore wind turbine established by [4] was used to develop an active control strategy. An ATMD combined with a robust control system has been proposed to reduce the nacelle/tower top fore-aft vibration. An optimal control scheme that makes use of the robust LQR feedback controller combined with a LQ state observer was proposed to find the ATMD actuator control force. The LQ state observer was designed in a way to reconstruct the complete state space information based on the measured output. Based on the obtained numerical results, it is shown that the proposed control scheme is effective at reducing the nacelle/tower vibration. Peak-to-peak reduction up to 21%, 40% and 30% (and RMS up to 30%, 67% and 44.5%) were achieved for LC4, LC6 and LC14 respectively.

## ACKNOWLEDGEMENTS

This work was carried out within the framework of the WEAMEC, West Atlantic Marine Energy Community, and the funding from the CARENE, Communauté d'Agglomération de la Région Nazairienne et de l'Estuaire.

## REFERENCES

- [1] Zuo, Haoran; Bi, Kaiming; Hao, Hong. "A state-of-the-art review on the vibration mitigation of wind turbines." *Renewable and Sustainable Energy Reviews* Vol. 121(2020): 109710, ISSN 1364-0321. <https://doi.org/10.1016/j.rser.2020.109710>.
- [2] Lackner, Matthew; Rotea, Mario. "Passive structural control of offshore wind turbines." *Wind Energy* Vol. 14 No. 3(2011): pp. 373-388. <https://doi.org/10.1002/we.426>
- [3] Zuo, Haoran; Bi, Kaiming; Hao, Hong. "Using multiple tuned mass dampers to control offshore wind turbine vibrations under multiple hazards" *Engineering Structures* Vol. 141 (2017): pp. 303-315. <https://doi.org/10.1016/j.engstruct.2017.03.006>
- [4] Sun, Chao. "Semi-active control of monopile offshore wind turbines under multi-hazards." *Mechanical Systems and Signal Processing* Vol. 99 (2018): pp. 285-305. <https://doi.org/10.1016/j.ymsp.2017.06.016>
- [5] Sun, Chao. "Mitigation of offshore wind turbine responses under wind and wave loading: Considering soil effects and damage." *Structural Control and Health Monitoring* Vol. 25 (2018): e2117. <https://doi.org/10.1002/stc.2117> ]
- [6] Fitzgerald, Breiffni; Basu, Biswajit. "Structural control of wind turbines with soil structure interaction included." *Engineering Structures* Vol. 11 (2016): pp. 131-151. <https://doi.org/10.1016/j.engstruct.2015.12.019>
- [7] Fitzgerald, Breiffni; Sarkar, Saptarshi; Staino, Andrea. "Improved reliability of wind turbine towers with active tuned mass dampers (ATMDs)." *Journal of Sound and Vibration* Vol. 419(2018): pp. 103-122. <https://doi.org/10.1016/j.jsv.2017.12.026>
- [8] M. Brodersen et al, Active tuned mass damper for damping of offshore wind turbine vibrations, *Wind Energ.* 2017; 20:783–796

[9] Fitzgerald, Breiffni; Basu, Biswajit; Nielsen, Søren R.K. “Active tuned mass dampers for control of in-plane vibrations of wind turbine blades.” *Structural Control and Health Monitoring* Vol. 20 No.12 (2013): pp: 1377-1396. <https://doi.org/10.1002/stc.1524>

[10] Lackner, M.A. and Rotea, M.A. (2011b) ‘Structural control of floating wind turbines’, *Mechatronics*, Vol. 21, No. 4, pp.704–719.

[11] Kwakernaak, Huibert and SIVAN, Raphael. “Linear Optimal Control Systems.” *Wiley-Interscience*, New York, (1972)

[12] Jonkman, J.M and Buhl, M.L. “FAST User’s Guide.” Technical Report NREL/TP-500-3820 National Renewable Energy Laboratory 2005.

[13] Bak, Christian; Zahle, Frederik; Bitsche, Robert; Kim, Taeseong; Yde, Anders; Henriksen, Lars Christian; Natarajan, Anand and Hansen, Morten. “Description of the DTU 10 MW reference wind turbine.” DTU Wind Energy Report-I-0092. STU Wind Energy. July 2013. <https://dtu-10mw-rwt.vindenergi.dtu.dk>

[14] Gunjit, Bir. “User’s Guide to BModes” National Renewable Energy Laboratory 2007.

[15] Alkhoury P, Soubra A-H, Rey V, Aït-Ahmed M. A full three-dimensional model for the estimation of the natural frequencies of an offshore wind turbine in sand. *Wind Energy*. 2021;24:699–719. <https://doi.org/10.1002/we.2598>

[16] Ghosh, Basu and Basu Biswajit. “A closed-form optimal tuning criterion for TMD in damped structures.” *Structural Control and Health Monitoring*. Vol. 14 No. 4 (2007): pp. 681-692. <https://doi.org/10.1002/stc.176>

[17] Bakre S.V. and Jangid R.S. “Optimum parameters of tuned mass damper for damped main system” *Structural Control and Health Monitoring*. Vol. 14 No. 3 (2007): pp. 448-470. <https://doi.org/10.1002/stc.166>

[18] Fischer T; De Vries, W.E; Schmidt, B. “Upwind design basis WP4: Offshore foundations and support structures” 2010. <http://resolver.tudelft.nl/uuid:a176334d-6391-4821-8c5f-9c91b6b32a27>